The Journal of Toxicological Sciences (J. Toxicol. Sci.)
Vol.36, No.1, 95-100, 2011

Letter

Effects of coating materials and size of titanium dioxide particles on their cytotoxicity and penetration into the cellular membrane

Tadashi Uchino, Yoshiaki Ikarashi and Tetsuji Nishimura

Division of Environmental Chemistry, National Institute of Health Sciences, 1-18-1 Kamiyoga, Setagaya-ku, Tokyo 158-8501, Japan

(Received August 6, 2010; Accepted October 15, 2010)

ABSTRACT — In order to estimate the effects of the size and surface treatment (coating or non-coating) of titanium dioxide particles on their cytotoxicity and penetration into the cellular membrane, two types of non-treated titanium dioxide (TiO_2) particles of 20 nm (LU175) and 250 nm (LU205) were exposed to CHO cells, RBL-2H3 cells, A431 cells, B16 melanoma, NHEK(F), and NHSF, and six types of surface-treated or non-treated TiO_2 particles of 35 nm were exposed to RBL-2H3 cells and NHSF. The order of half-maximal inhibitory concentrations (IC50s) of LU175 was NHSF < CHO, RBL-2H3 < A431 < B16 melanoma, NHEK(F). On the other hand, LU205 showed no cytotoxicity against any cells. Surface-treated TiO_2 showed much less cytotoxicity against RBL-2H3 cells than non-treated TiO_2. Then, between 0.5 and 10 mg of LU175 or LU205 was exposed to CHO cells. After 24 hr, the amount of LU175 in cellular cytosol increased dose-dependently. On the other hand, the amount of LU205 in cellular cytosol was much less than that of LU175. The proportion of surface-treated TiO_2 in the cellular cytosol of RBL-2H3 cells differed for each coating material. These results suggested that TiO_2 has different cytotoxicities among cell lines, and that of surface-treated TiO_2 was weaker than that of non-treated TiO_2. TiO_2 located in cytosol might be the main cause of cytotoxicity.

Key words: Nanomaterials, Titanium dioxide, Cytotoxicity, Penetration, RBL-2H3 cells, NHSF

INTRODUCTION

In recent years, the use of nanomaterials such as titanium dioxide (TiO_2) in cosmetics such as sunscreen has advanced rapidly without adequate evaluation of their safety (Ishii, 2005; Hatakeyama, 2005; Lovern and Klaper, 2006; Xia *et al.*, 2006). Hussain *et al.* (2005) demonstrated that TiO_2 (40 nm) at higher doses (100-250 μg/ml) did not induce significant cytotoxicity against BRL 3A rat liver cells, while silver nanoparticles at lower doses (10-50 μg/ml) induced significant cytotoxicity against the cells. Reeves *et al.* (2008) demonstrated that TiO_2 (anatase, 5 nm) at 1,000 μg/ml induced slight cytotoxicity against goldfish skin cells without Ultraviolet-A(UVA)-irradiation. On the other hand, Sayes *et al.* (2006) demonstrated that nanoscale TiO_2 at 100 μg/ml induced significant cytotoxicity and inflammation against human dermal fibroblasts and human lung epithelial cells. Onuma *et al.* (2009) demonstrated that nano-sized TiO_2 had strong cytotoxicity against mouse fibrosarcoma cells. However, few reports about cytotoxicity of nano-sized TiO_2. In particular, little is known about cytotoxicity of nano-sized TiO_2 against various kinds of cells. Thus, it was considered necessary to compare cytotoxicity of nano-sized TiO_2 among various kinds of cells to estimate the potential toxicity of TiO_2. In order to estimate the toxicity of TiO_2, we examined the cytotoxicity of two kinds of non-coating rutile form TiO_2 with particle sizes of 20 nm (LU175) and 250 nm (LU205) against various kinds of cells and transferred LU175 and LU205 into the cellular components.

Surfaces of TiO_2 are usually coated with SiO_2, $Al(OH)_3$, Al_2O_3, or silicone for use in cosmetics. Warheit *et al.* (2007) demonstrated that surface-treated material affects TiO_2 toxicity against rat lung. However, there are few reports investigating the cytotoxic effects of coating materials on cells and the penetration of TiO_2 into cellular components. We examined the cytotoxicity of surface-treated and non-treated TiO_2 against cultured cells and

Correspondence: Tadashi Uchino (E-mail: uchino@nihs.go.jp)

transferred TiO_2 into the cellular components.

MATERIALS AND METHODS

Cells

C57BL/6 mouse melanoma (B16 melanoma), Chinese hamster ovary (CHO) cells, and rat basophilic leukemia (RBL-2H3) cells were purchased from Health Science Research Resources Bank (Osaka, Japan). Normal human skin fibroblasts (NHSF) and human epidermoid carcinoma (A431) cells were purchased from Riken Bioresources Center Cell Bank (Ibaraki, Japan). Normal human epidermis keratinocytes from neonatal foreskin (NHEK(F)) were purchased from Kurabo Industries Ltd. (Osaka, Japan).

Culture medium

Eagle's-MEM containing 10% FBS was used as culture medium for B16 melanomas, CHO cells and RBL-2H3 cells. Epi-Life KG2 was used as culture medium for A431 cells and NHEK(F). α-MEM containing 10% FBS was used as culture medium for NHSF.

Particles

Non-coating materials

LU175 and LU205 were obtained from Isihara Sangyo Kaisha, Ltd. (Osaka, Japan). TiO_2 (rutile form) particles of 35 nm (MT-500B: TiO_2 96%) were obtained from Teika Co. (Osaka, Japan).

Coating materials

TiO_2 (rutile form) particles of 35 nm coated with $Al(OH)_3$ and stearic acid (TTO-55(C): TiO_2 90%) and such particles coated with $Al(OH)_3$ (TTO-55(A); TiO_2 96%) were obtained from Isihara Sangyo Kaisha, Ltd. TiO_2 (rutile form) particles of 35 nm coated with $Al(OH)_3$, SiO_2, and silicone (SMT-500SAS: TiO_2 80%), such particles coated with $Al(OH)_3$ and SiO_2 (MT-500SA; TiO_2 85%), and such particles coated with Al_2O_3 (MT-500H: TiO_2 90%) were obtained from Teika Co.

Microwave digestion

After collecting cellular membrane, microsome, and cytosol, these components were added to teflon vessels, and then 5 ml of HNO_3 was added to each vessel. Then, the vessel contents were digested for 22 min (up to 80 PSI for 20 min, maintained for 2 min) using a microwave (MARS 5, CEM Co., Matthews, NC, USA).

ICP-MS measurement

The digested solution was diluted 5 times with milli-Q water and Ti contents were determined by ICP-MS (HP-4500, Hewlett-Packard Co., Palo Alto, CA, USA). ICP-MS conditions were as follows:

RF power:1450 W, RF refraction current: 5 W

Monitoring mass: m/z 48 (Ti)

Cytotoxicity

B16 melanomas, CHO cells, and RBL-2H3 cells were suspended in 0.1 ml of culture medium at a concentration of 5×10^4 cells/ml. A431 cells and NHEK(F) were suspended in 0.1 ml of culture medium at concentrations of 4×10^4 cells/ml and 5×10^4 cells/ml, respectively. NHSF was suspended in 0.1 ml of culture medium at a concentration of 4×10^4 cells/ml. All cells were seeded in a 96-well microplate and cultured for 2 days for CHO cells, 5 days for A431 cells, or 3 days for other cells under 5% CO_2 at 37°C.

TiO_2 particles were suspened in culture medium and ultrasonicated for 5 min. Immediately after ultrasonication, culture medium in the each microplate were removed and suspension (0.1 ml) of LU175 or LU205, the concentration of which ranged from 0 to 10 mg/ml, was added to each well. After 24 hr, cells were washed 5 times with medium and then for the viability assay, 0.1 ml of tetra-color one dissolved in medium was added, followed by incubation for 2 hr. Tetra -color one is a mixture of water-soluable tetrazolium solt [2-(2-Methoxy-4-nitrophenyl)-3-(4-nitorophenyl)-5-(2,4-disulfophenyl)-2H-tetrazolium, monosodium salt)] and electron carrier (1-Methoxy-5-methylphenazinium methylsulfate) converted to a water-soluable formazan by dehydrogenase enzymes located mainly in the mitochondria of living cells. Absorbance at 490 nm (reference at 650 nm) was measured with a microplate reader (Spectramax M5, Molecular Devices Co., Tokyo, Japan) and the half-maximal inhibitory concentration of viability (IC50) was derived.

TiO_2 transferred into cellular components

Five ml of cell suspension of CHO cells and RBL-2H3 cells (5×10^4 cells/ml) or NHSF cells (4×10^4 cells/ml) was cultured in a 60-mm dish for 2 days under 5% CO_2 at 37°C. After removing the medium, 5 ml of 0.1 or 0.5 or 2 mg/ml TiO_2 suspened in culture medium was added and the mixture was incubated for a further 24 hr. After washing cells 5 times with medium, the cells were treated with trypsin and collected. The cells were suspended in 1.5 ml of phosphate-buffered saline (PBS) and ultrasonicated for 5 min. Then, cell suspensions were cell-fractionated in accordance with the scheme shown in Fig.1 and the

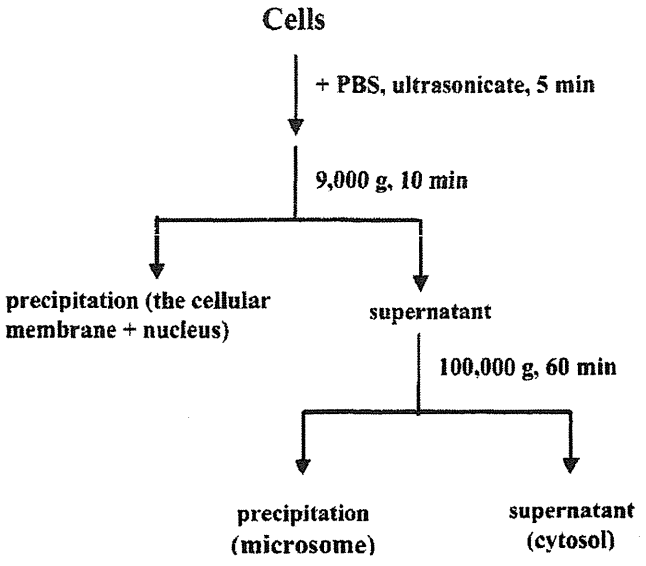

Fig. 1. Method of cell fractionation.

levels of Ti in the cellular membrane (including nucleus), microsome, and cytosol were determined by ICP-MS.

Statistical analysis

Differences between A431 and NHSF, CHO, or RBL-2H3 group, non-coated TiO_2 treatment group, and surface-treated TiO_2 treatment group were examined by Student's t-test. The differences were considered significant at $P < 0.05$.

RESULTS

Cytotoxicity of TiO_2 against cultured cells

LU175 showed cytotoxicity against NHSF, CHO, and RBL-2H3. On the other hand, LU175 showed no cytotoxicity against A431, B16 melanoma, and NHEK(F). IC50s of LU175 against NHSF, CHO, and RBL-2H3 were significantly decreased from that of the A431 group. LU205 showed no cytotoxicty against any cells (Table 1). IC50s of surface-treated TiO_2 were significantly higher than those of non-treated TiO_2 against NHSF and RBL-2H3 cells (Table 2).

Transfer of TiO_2 into the cellular components

500-10,000 μg of LU175 or LU205 was added to a culture of CHO cells in a 60-mm dish. After 24 hr, over 99% of LU205 was located in the cellular membrane, while 88.5-96.7% and 3.3-11.3% of LU175 were located in cellular membrane and cytosol, respectively (Table 3). The proportion of LU175 located in the cytosol was significantly increased from that in the LU205 group (Table 3).

The suspensions of 100 μg/ml surface-treated and non-treated TiO_2 were added to the NHSF seeded in a 60-mm dish. In non-treated TiO_2, proportions of MT-500B and LU175 located in cytosol were significantly increased from that in the LU205 group (Table 4). In surface-treated TiO_2, proportions of TTO-55(C) and SMT-500SAS located in cytosol were significantly increased from that in the MT-500SA group (Table 4). Similar results were obtained for RBL-2H3 cells (Table 4).

DISCUSSION

Xu *et al.* (2010) reported that nano-scale TiO_2 was administered to wild-type rat by a novel intrapulmonary spraying five times over 9 days, 8-hydroxyguanosine level and superoxide dismutase activity expression in the lung. Gurr *et al.* (2005) and Onuma *et al.* (2009) reported that reactive oxygen generated from TiO_2 in the dark induced cytotoxicity. Thus, the mechanism of the cytotoxicity of LU175 might be through reactive oxygen generated from TiO_2 in the dark. However, it was not clear that the kind of reactive oxygen generated from TiO_2 in the dark. Therefore, further study should be carried out.

Table 1. Cytotoxicity of LU175 and LU205 against various cells

Cell	IC50 (mg/ml)	
	LU175	LU205
CHO	1.3 ± 0.3*	> 10
RBL-2H3	1.4 ± 1.0*	8.6 ± 1.2
NHSF	0.5 ± 0.2**	> 10
A431	8.3 ± 2.9	7.0 ± 2.6
NHEK (F)	> 10	> 10
B16 melanoma	> 10	> 10

Data are means ± S.D. of three experiments. Significantly different from A431 group. *$P < 0.05$. **$P < 0.01$.

Table 2. Cytotoxicity of TiO_2 against NHSF and RBL-2H3 cells

	IC50 (mg/ml)	
	NHSF	RBL-2H3
SMT-500SAS	4.6 ± 0.4***	4.9 ± 1.9*
MT-500SA	> 10	> 10
MT-500H	> 10	5.9 ± 1.4**
TTO-55 (C)	2.1 ± 1.5	2.3 ± 1.4
TTO-55 (A)	> 10	> 10
MT-500B	0.12 ± 0.04	0.6 ± 0.4

Data are means ± S.D. of three experiments. Significantly different from MT-500B group, *$P < 0.05$, **$P < 0.01$, ***$P < 0.001$.

Table 3. The distribution of different particle sizes of TiO_2 in the cellular components of CHO cells

	Exposed (μg)	Detected (μg: mean ± S.D. n = 3)		
		Membrane	Microsome	Cytosol
LU175	500	83 ± 3	ND (< 0.004)	4.1 ± 2.7
		(95.3 ± 3.4%)	(0.0%)	(4.7 ± 3.1%)
	2500	176 ± 15	ND	6.0 ± 2.4*
		(96.7 ± 8.2%)	(0.0%)	(3.3 ± 1.3%*)
	10000	133 ± 17	0.28 ± 0.12	17 ± 14
		(88.5 ± 11.3%)	(0.2 ± 0.08%)	(11.3 ± 9.3%)
LU205	500	416 ± 8	2.4 ± 0.7	0.050 ± 0.001
		(99.41 ± 1.91%)	(0.57 ± 0.17%)	(0.02 ± 0.0004%)
	2500	1238 ± 25	3.6 ± 1.1	0.05 ± 0.08
		(99.71 ± 2.01%)	(0.29 ± 0.09%)	(0.004 ± 0.007%)
	10000	5395 ± 836	0.28 ± 0.11	0.61 ± 0.08
		(99.98 ± 15.49%)	(0.005 ± 0.002%)	(0.01 ± 0.001%)

The data detected after 24-hr exposure of TiO_2 onto CHO cells. Significantly different from LU205 group. *$P < 0.05$.

The cell size of NHSF, CHO, and RBL-2H3 cells were larger than B16 melanoma, A431 cells, and NHEK(F). Therefore, it was speculated that the cytotoxicity of LU175 might be connected to cell size. Surface-treated TiO_2 showed less cytotoxicity against RBL-2H3 cells and NHSF than non-treated TiO_2.

These results suggested that surface treatment with coating materials would reduce the surface reactive activity of TiO_2 and thus reduce its cytotoxicity. On the other hand, the cytotoxicity of surface-treated TiO_2 depends on the kind of coating material. The cytotoxicities of coating materials themselves are not known, so further study should be carried out.

Dose-dependent levels of LU175 were present in the cytosol of CHO cells. MT-500B and LU175 located in the cytosol of NHSF and RBL-2H3 cells were significantly increased from those in the LU205 group (Tables 3 and 4).

These results suggested that non-coating TiO_2 locat-

Table 4. Influence of surface coating on the distribution of TiO_2 in the cellular components of NHSF and RBL-2H3 cells

(a) NHSF (unit: μg)

TiO_2 500 μg	SMT-500SAS	MT-500SA	MT-500H	TTO-55(C)	TTO-55(A)	MT-500B	LU175	LU205
Cellular membrane	15.8 ± 1.4	117 ± 4	68.5 ± 3.8	3.55 ± 0.04	76.0 ± 2.3	83.2 ± 4.7	84 ± 5	426 ± 26
Microsome	0.26 ± 0.17	3.89 ± 0.26	0.92 ± 0.20	1.88 ± 0.06	ND	2.64 ± 0.24	23 ± 13	ND
Cytosol	1.92 ± 0.11	0.43 ± 0.04	2.85 ± 0.18	2.98 ± 0.18	0.59 ± 0.01	0.72 ± 0.07	2.8 ± 1.6	1.0 ± 0.7

(mean ± S.D., n = 3)

(presence ratio: %)

TiO_2 500 μg	SMT-500SAS	MT-500SA	MT-500H	TTO-55(C)	TTO-55(A)	MT-500B	LU175	LU205
Cellular membrane	87.88 ± 7.78	96.44 ± 3.30	94.78 ± 5.26	42.2 ± 0.5$^{\#\#}$	99.23 ± 3.00	96.11 ± 5.43	76.4 ± 4.6**	99.8 ± 6.1
Microsome	1.45 ± 0.95	3.21 ± 0.21	1.27 ± 0.28	22.4 ± 0.7	ND	3.05 ± 0.27	20.9 ± 11.8	ND
Cytosol	10.67 ± 0.61$^{\#\#\#}$	0.35 ± 0.03	3.95 ± 0.25	35.4 ± 2.1$^{\#\#\#}$	0.77 ± 0.01	0.84 ± 0.08**	2.5 ± 1.5	0.20 ± 0.16

(mean ± S.D., n = 3)

(b) RBL-2H3 (unit: μg)

TiO_2 500 μg	SMT-500SAS	MT-500SA	MT-500H	TTO-55(C)	TTO-55(A)	MT-500B	LU175	LU205
Cellular membrane	36.9 ± 18.7	283 ± 63	116 ± 48	32.0 ± 22.2	73.9 ± 5.8	89.3 ± 23.3	383 ± 39	471 ± 71
Microsome	0.24 ± 0.12	3.1 ± 1.5	1.3 ± 0.3	0.18 ± 0.27	0.91 ± 0.41	0.53 ± 0.17	3.1 ± 0.4	6.1 ± 0.6
Cytosol	0.63 ± 0.08	1.10 ± 0.06	3.61 ± 0.14	1.17 ± 0.09	0.86 ± 0.03	0.79 ± 0.06	0.54 ± 0.11	0.17 ± 0.13

(mean ± S.D., n = 3)

(presence ratio: %)

TiO_2 500 μg	SMT-500SAS	MT-500SA	MT-500H	TTO-55(C)	TTO-55(A)	MT-500B	LU175	LU205
Cellular membrane	97.7 ± 49.5	98.54 ± 21.94	95.94 ± 39.70	95.95 ± 66.57	97.66 ± 7.66	98.54 ± 25.71	99.05 ± 10.09	98.69 ± 14.88
Microsome	0.64 ± 0.32	1.08 ± 0.52	1.08 ± 0.25	0.54 ± 0.81	1.22 ± 0.54	0.58 ± 0.32	0.81 ± 0.10	1.27 ± 0.13
Cytosol	1.66 ± 0.21$^{\#\#\#}$	0.38 ± 0.02	2.98 ± 0.12	3.51 ± 0.27$^{\#\#}$	1.14 ± 0.04	0.87 ± 0.07***	0.14 ± 0.03*	0.04 ± 0.03

(mean ± S.D., n = 3)

Significantly different from LU205 group, *P < 0.05, **P < 0.01, ***P < 0.001
Significantly different from MT-500SA group, $^{\#\#}$P < 0.001.

ed in the cytosol might be the main cause of cytotoxicity. Since the distribution in the cytosol of surface-treated TiO_2 is at the same level or higher than that of non-coating TiO_2, the distribution in the cytosol of surface-treated TiO_2 might not be the cause of the cytotoxicity of TiO_2. Since the distributions in the cytosol of TTO-55(C) and SMT-500SAS were significantly increased from that in the MT-500SA group, stearic acid or silicone induced the distribution in the cytosol.

ACKNOWLEDGMENTS

We thank Isihara Sangyo Kaisha, Ltd. for generously donating LU175, LU205, TTO-55(C), and TTO-55(A) and Teika Co. for generously donating MT-500B, SMT-500SAS, MT-500SA, and MT-500H.

REFERENCES

Gurr, J., Wang, A.S.S., Chen, C. and Jan, K. (2005): Ultrafine titanium dioxide particles in the absence of photoactivation can induce oxidative damage to human bronchial epithelial cells. Toxicology, **213**, 66-73.

Hatakeyama, Y. (2005): Safety evaluation of the nanoparticles on cosmetics. Journal of Japanese Cosmetic Science Society, **29**, 225-231.

Hussain, S.M., Hess, K.L., Gearhart, J.M., Geiss, K.T. and Schlager, J.J. (2005): *In vitro* toxicity of nanoparticles in BRL 3A rat liver cells. Toxicol. In Vitro, **19**, 975-983.

Ishii, H. (2005): Development of water resistant sunscreening agent using nano-technology. Journal of Japanese Cosmetic Science Society, **29**, 215-220.

Lovern, S.B. and Klaper, R. (2006): Daphnia magna mortality when exposed to titanium dioxide and fullerene (C60) nanoparticles. Environmental Toxicol. Chem., **25**, 1132-1137.

Onuma, K., Sato, Y., Ogawara, S., Shirasawa, N., Kobayashi, M., Yoshitake, J., Yoshimura, T., Iigo, M., Fujii, J. and Okada, F. (2009): Nano-scaled particles of titanium dioxide convert benign mouse fibrosarcoma cells into aggressive tumor cells. Am. J. Pathol., **175**, 2171-2183.

Reeves, J.F., Davies, S.J., Dodd, N.J. and Jha, A.N. (2008): Hydroxyl radicals ($^{\bullet}OH$) are associated with titanium dioxide (TiO_2) nanoparticle-induced cytotoxicity and oxidative DNA damage in fish cells. Mutat. Res., **640**, 113-122.

Sayes, C.M., Wahi, R., Kurian, P.A., Liu, Y., West, J.L., Ausman, K.D., Warheit, D.B. and Colvin, V.L. (2006): Correlating nanoscale titania structure with toxicity: a cytotoxicity and inflammatory response study with human dermal fibroblasts and human lung epithelial cells. Toxicol. Sci., **92**, 174-185.

Warheit, D.B., Webb, T.R., Reed, K.L., Frerichs, S. and Sayes, C.M. (2007): Pulmonary toxicity study in rats with three forms of ultrafine-TiO_2 particles: differential responses related to surface properties. Toxicology, **230**, 90-104.

Xia, T., Kovochich, M., Brant, J., Hotze, M., Sempf, J., Oberley, T., Sioutas, C., Yeh, J.I., Wiesner, M.R. and Nel, A.E. (2006): Comparison of the abilities of ambient and manufactured nanoparticles to induce cellular toxicity according to an oxidative stress paradigm. Nano Lett., **6**, 1794-1807.

Xu, J., Futakuchi, M., Iigo, M., Fukamachi, K., Alexander, D.B., Shimizu, H., Sakai, Y., Tamano, S., Furukawa, F., Uchino, T., Tokunaga, H., Nishimura, T., Hirose, A., Kanno, J. and Tsuda, H. (2010): Involvement of macrophage inflammatory protein 1α(MIP1α) in promotion of rat lung and mammary carcinogenic activity of nanoscale titanium dioxide particles administered by intra-pulmonary spraying. Carcinogenesis, **31**, 927-935.

Enhancement of tongue carcinogenesis in Hras128 transgenic rats treated with 4-nitroquinoline 1-oxide

KUNIKO NAOI[1], NAO SUNAGAWA[2], ICHIRO YOSHIDA[1], TAKAMITSU MORIOKA[2], MAKOTO NAKASHIMA[1], MASASHI ISHIHARA[1,3], KATSUMI FUKAMACHI[4], YOSHINORI ITOH[3], HIROYUKI TSUDA[4], NAOKI YOSHIMI[2] and MASUMI SUZUI[1]

[1]Department of Medical Therapeutics and Molecular Therapeutics, Gifu Pharmaceutical University, 5-6-1 Mitahora-higashi, Gifu 502-8585; [2]Tumor Pathology Division, University of the Ryukyus Faculty of Medicine, 207 Uehara, Nishihara-cho, Okinawa 903-0215; [3]Department of Pharmacy, Gifu University Hospital, 1-1 Yanagido, Gifu 501-1194; [4]Department of Molecular Toxicology, Graduate School of Medical Sciences, Nagoya City University, 1 Kawasumi, Mizuho-cho, Mizuho-ku, Nagoya 467-8601, Japan

Received September 3, 2009; Accepted October 29, 2009

DOI: 10.3892/or_00000641

Abstract. Transgenic rats carrying human c-Ha-*ras* proto-oncogene (Hras128 rats) have been shown to be highly susceptible to induction of tumors. We have found an early induction of tongue tumors in Hras128 rats treated with 4-nitroquinoline 1-oxide (4NQO). 4NQO was administered to the Hras128 and wild-type Sprague-Dawley (SD) rats for 4 and 8 weeks, respectively. The experiment was terminated at 14 (Hras128 rats) and 28 (SD rats) weeks. Either during or after treatment with 4NQO, dysplastic hyperplasia, papilloma and squamous cell carcinoma were found on the tongue of both Hras128 and wild-type rats, with a higher incidence and multiplicity in Hras128 rats. Treatment of the Hras128 rats with 4NQO significantly increased cell proliferation in the tumor compared to the control rats. In the tongue tumors of the Hras128 rats, there was a significant increase in the mRNA expression levels of cyclin D1 and COX2. To examine whether this experimental system is useful for screening of the candidate agents for cancer preventive effect, nimesulide, a selective COX2 inhibitor, was tested in the present model. Nimesulide significantly decreased total multiplicity of tongue lesions compared to the control rats. Treatment of Hras128 rats with nimesulide caused a significant decrease in the levels of mRNA expression of cyclin D1 and COX2 in the tumor. Therefore, the current 4NQO-induced Hras128 rat tongue carcinogenesis model provides a simple and rapid system for investigating carcinogenesis process and evaluating the effect of possible cancer preventive agents for human tongue cancer.

Correspondence to: Dr Masumi Suzui, Department of Medical Therapeutics and Molecular Therapeutics, Gifu Pharmaceutical University, 5-6-1 Mitahora-higashi, Gifu 502-8585, Japan
E-mail: suzui@gifu-pu.ac.jp

Key words: tongue carcinogenesis, *ras*, transgenic rat, 4-nitroquinoline 1-oxide

Introduction

Oral cancer is a relatively common malignancy ranking 11th in frequency on a worldwide basis, and more than 390,000 new cases are being diagnosed annually (1,2). Human oral cancer is related to cigarette smoking and chewing or smokeless tobacco (3). This disease has a multifocal character often referred to as a field cancerization (4). This malignancy is most common in developing countries of Asia and South America (5), and incidence and mortality rate of this disease are rising in developed countries, especially in young males (6-8). This aggressive epithelial malignancy is associated with severe morbidity and poor survival despite recent advances in treatment (7).

Rat model using 4-nitroquinoline 1-oxide (4NQO) has been widely used for investigating carcinogenesis of oral cancer and evaluating the modulatory effects of possible chemopreventive agents (9,10). The 4NQO-induced oral cancer is derived from papilloma through hyperplastic epithelium and dysplasia (11), and this multistage process mimics the development of these malignancies in human (11,12). Recent reports by Tsuda and his colleagues demonstrate that transgenic rat carrying human c-Ha-*ras* proto-oncogene, termed Hras128 rat [Jcl/SD-TgN(HrasGen)128Ncc], is highly susceptible to tumor induction in various organ sites including mammary gland, esophagus, skin, urinary bladder and tongue (13-15).

In the present study, we developed a novel tongue carcinogenesis Hras128 rat model by using 4NQO to cause a rapid induction of tongue tumors within as short a period as 14 experimental weeks. Using this experimental system, we also confirmed that nimesulide, a selective COX2 inhibitor, which has been demonstrated to prevent rat tongue carcinogenesis (16), prevents the occurrence of tongue tumors induced with 4NQO.

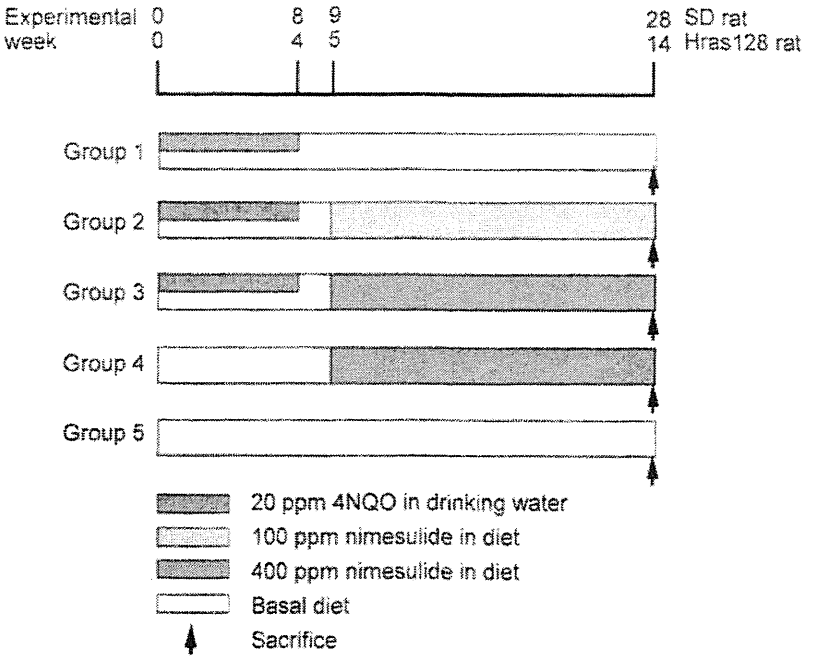

Figure 1. Experimental protocol. As indicated, the experimental period of the Hras128 and wild-type SD rat lasted 14 and 28 weeks, respectively.

Materials and methods

Animals. A total of 80 male Hras128 rats [Jcl/SD-TgN (HrasGen)128Ncc] and wild-type Sprague-Dawley (SD) rats bred by CLEA (CLEA Japan, Inc., Tokyo, Japan) at 6 weeks old were maintained in plastic cages in a conditioned room at 23±2°C, 50±10% humidity and 12-h light/dark cycle lighting. The animals were allowed free access to powdered basal diet CE-2 (CLEA Japan) and tap water. The animals were also maintained in the Animal Facility of University of the Ryukyus, Faculty of Medicine, and the experiments were conducted according to the Institutional Animal Care Guidelines of University of the Ryukyus.

Treatment. After one week of acclimatization, rats were randomly assigned to the experimental groups (Fig. 1). Hras128 and SD rats in groups 1-3 (10 rats each) were given tap water containing 20 ppm 4NQO (CAS no. 56-57-5, Wako Pure Chemical, Osaka, Japan; 98% pure) for 4 and 8 weeks, respectively. One week after 4NQO treatment, rats in groups 2 and 3 received 100 and 400 ppm nimesulide (CAS no. 51803-78-2, Nacalai Tesque, Inc., Kyoto, Japan) in basal diet until the end of the experiment, and rats in group 1 received no further treatment and fed the basal diet. Rats in group 4 received the 400 ppm nimesulide diet without 4NQO treatment. Rats in group 5 were fed the basal diet alone and served as untreated controls. Careful observation of tongue lesions was done on a weekly basis until the end of the experiment. Animals were weighed weekly and consumption of the experimental diets was also recorded. Tongue lesions including dysplastic hyperplasia (DH), papilloma (PAP) and squamous cell carcinoma (SCC) were noted grossly for their location, number, and size, and tumor incidence and multiplicity were analyzed. At 14 and 28 weeks after the start of the experiment, Hras128 and SD rats were euthanized with CO_2 anesthesia, and then complete autopsies were performed with these animals. The identified tumors were carefully removed and cut into two segments. One segment of the tumor was immediately frozen in liquid nitrogen for reverse transcription-PCR (RT-PCR) analysis: the second segment was fixed in 10% buffered formalin and then processed for histopathological (hematoxylin and eosin staining) and immunohistochemical analyses. Oral lesions including dysplasia and neoplasia were diagnosed according to the criteria described elsewhere (17,18).

Immunohistochemical staining and measurement of PCNA positive index. These assays were performed using an established method as previously described by us (19). In brief, 4-μm thick paraffin sections were prepared to include the tongue tumor or adjacent normal mucosa. These sections were treated in 3% H_2O_2 for 20 min to block the endogenous peroxidase activity and then incubated with a primary antibody of proliferating cell nuclear antigen (PCNA) (1:50 dilution) (Dako Co., Ltd., Kyoto, Japan) at room temperature for 60 min. Sections were then stained using a Simple Stain kit (Nichirei, Tokyo, Japan) according to the manufacturer's instructions. PCNA was measured in cells consisting of the tongue tumor or normal mucosa. The PCNA positive index was determined by calculating the ratio of PCNA-positive nuclei/total number of nuclei counted as described by us (19). More than 300 cells were counted in each lesion.

Reverse transcription-PCR (RT-PCR) analysis. These assays were performed by established procedures (20). Snap-frozen

Table I. Body, liver, kidney and relative liver weights in Hras128 rats.

Group	Treatment	No. of rats	Body weight (g)	Liver weight (g)	Kidney weight (g)	Relative liver weight (g/100 gr body weight)
1	4NQO	10	597±30[a,b]	24.6±2.9[b]	4.7±0.4	4.1±0.3[b]
2	4NQO→100 ppm nimesulide	10	577±24	22.4±3.1	4.6±0.4	3.8±0.4
3	4NQO→400 ppm nimesulide	10	531±42[b]	24.8±2.7	4.6±0.5	4.6±0.4[b]
4	400 ppm nimesulide	5	588±20	26.0±2.8	4.8±0.5	4.4±0.4
5	None	5	625±60[b]	28.0±4.8[b]	5.2±0.1	4.4±0.6

[a]Mean ± SD. [b]Statistically significant.

Table II. Body, liver, kidney and relative liver weights in Sprague-Dawley rats.

Group	Treatment	No. of rats	Body weight (g)	Liver weight (g)	Kidney weight (g)	Relative liver weight (g/100 gr body weight)
1	4NQO	8	523±100[a,b]	19.7±5.9	3.7±0.5[b]	3.7±0.8
2	4NQO→100 ppm nimesulide	10	520±77[b]	20.6±4.5	3.9±0.6	3.9±0.6[b]
3	4NQO→400 ppm nimesulide	10	538±29[b]	17.5±3.5[b]	3.6±0.4	3.2±0.5[b]
4	400 ppm nimesulide	5	662±96[b]	24.4±7.1[b]	5.0±0.8[b]	3.6±0.8
5	None	5	558±68	18.1±2.9	3.4±0.3	3.2±0.5[b]

[a]Mean ± SD. [b]Statistically significant.

histopathologically verified tongue tumors were randomly chosen and total RNA was extracted for RT-PCR assays. Total RNA was isolated from frozen tissues using a TRIzol reagent (Invitrogen Life Technologies, Inc., Rockville, MD) as recommended by the manufacturer. cDNA was amplified from total RNA (100 ng) using a SuperScript III One-Step RT-PCR System (Invitrogen Life Technologies). PCR was conducted for 35 or 38 cycles in a Takara PCR Thermal Cycler SP TP-400 (Takara Bio, Inc., Tokyo, Japan). The primers used for amplification were as follows: cyclin D1-specific primer set, CD-1F (5'-CTG GCC ATG AAC TAC CTG GA-3') and CD-1R (5'-GTC ACA CTT GAT GAC TCT GG-3'); p53-specific primer set, P-2F (5'-CAG CGA CAG GGT CAC CTA AT-3') and P-3R (5'-GTG GAT AGT GGT ATA GTC GG-3'); $p21^{CIP1}$-specific primer set, C-3F (5'-CCT TAG CCT TCA TTC AGT GT-3') and C-4R (5'-GCC AGG ATC AGA AAC ACA GC-3'); $p27^{KIPi}$-specific primer set, K-2F (5'-CCG CCT GCA GAA ACC TCT TC-3') and K-2R (5'-TGG ACA CTG CTC CGC TAA CC-3'); cyclooxygenase-2 (COX2)-specific primer set, PT-4F (5'-TGG GCC ATG GAG TGG ACT TA-3') and PT-4R (5'-ATG AGC CTG CTG GTT TGG AA-3'). ß-actin-specific PCR products for the same RNA samples were simultaneously amplified and served as internal controls. Primers BA-F2 (5'-GGG TAT GGG TCA GAA GGA CT-3') and BA-R2 (5'-TGT AGC CAC GCT CGG TCA GG-3') were used for amplification of ß-actin. Each amplification cycle consisted of 0.5 min at 94°C for denaturing, 0.5 min at 55°C for primer annealing and 1 min at 72°C for extension. PCR products were analyzed by agarose gel electrophoresis and stained with ethidium bromide. The results were confirmed by repeating experiments.

Statistical analysis. Tumor incidence and multiplicity were compared between the Hras128 and SD rats, or between animals treated with nimesulide and those not treated with nimesulide. Tumor incidence was analyzed by χ^2 or Fisher's exact probability test, and tumor multiplicity was analyzed by Student's or Welch's t-test. Significance was established at $P<0.05$.

Results

General observation. A total of 78 Hras128 and SD rats survived at the end of the experiment. Two SD rats in group 1 died from unidentified cause. No macroscopic metastases were observed in any of 78 rats. Body, liver, kidney and relative liver weights are shown in Tables I and II. In Table I, the body weight of group 3 was significantly lower than that

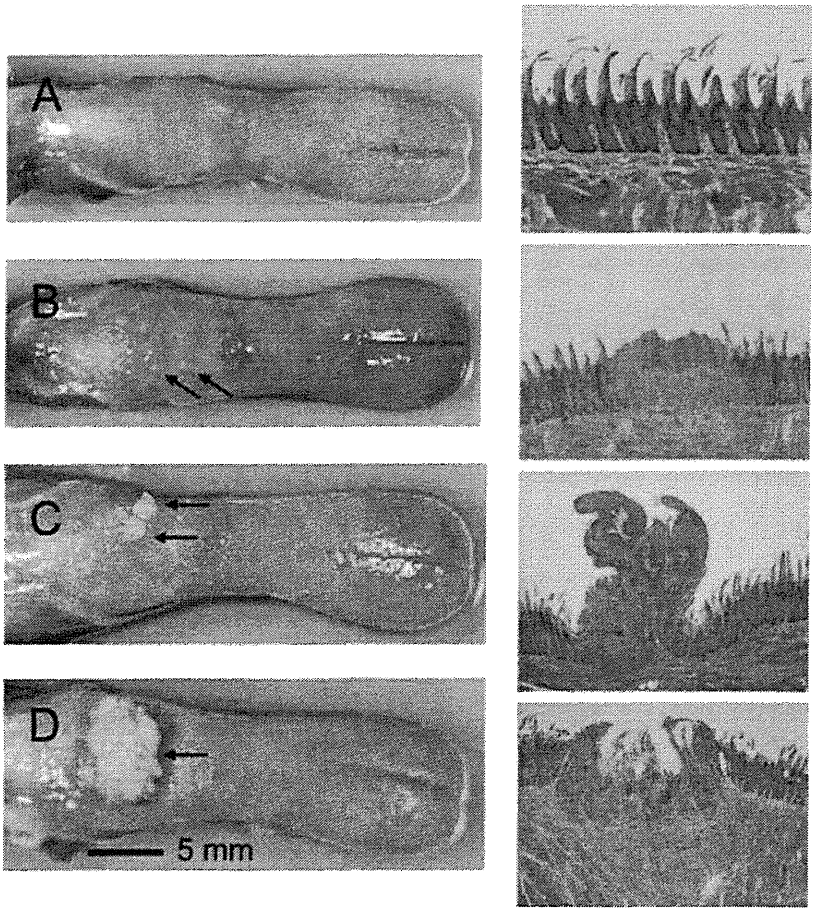

Figure 2. Macroscopic (left panels) and histological (right panels) appearance on the induced tongue lesions indicated by arrows. These lesions were induced with 4NQO in Hras128 rats. (A) Normal mucosa (N); (B) dysplastic hyperplasia (DH); (C) papilloma (PAP); (D) squamous cell carcinoma (SCC) (arrow). DH displayed thickened epithelium with prominent surface keratinization, loss of polarity in epithelial cells, nuclear pleomorphism, dyskeratosis and increased or abnormal mitosis. PAP and SCC exhibited non-invasive growth of neoplastic cells and invasive growth into subepithelial and muscular tissues, respectively.

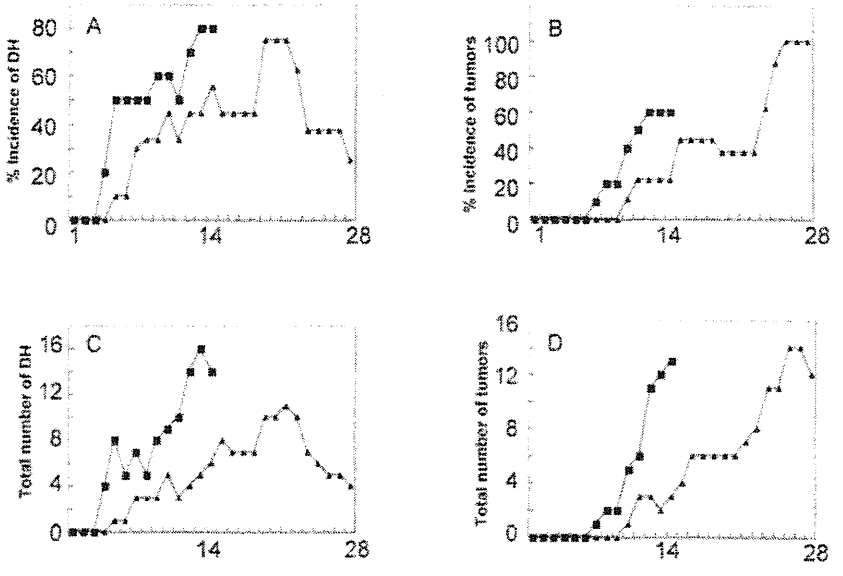

Figure 3. Occurrence of tongue lesions in Hras128 (closed square) and SD (closed triangle) rats. As indicated, left 2 panels indicate (%) incidence (A) and number (C) of dysplastic hyperplasia (DH). Note a marked increase in incidence and number of DH in Hras128 rats. This increase persisted until the end of the experiment (at experimental-week 14). Right 2 panels indicate (%) incidence (B) and number (D) of tumor. X-axis indicates the experimental week. Note that the incidence and number of tongue tumors (PAP and SCC) in the Hras128 rat are greater than that of the SD rat.

Table III. Incidence and multiplicity of the tongue lesions.

A. Hras128 rat

Group	Treatment	No. of rats	Incidence			Multiplicity		
			Total	DH	PAP+SCC	Total	DH	PAP+SCC
1	4NQO	10	8	8	6	3.4±2.1[a]	1.8±1.0	2.2±0.2
2	4NQO→100 ppm nimesulide	10	9	7	4	2.0±1.0	1.7±1.1	1.2±0.5
3	4NQO→400 ppm nimesulide	10	8	7	2[b]	1.6±0.7[c]	1.4±0.8	1.0±0.1
4	400 ppm nimesulide	5	0	0	0	0	0	0
5	None	5	0	0	0	0	0	0

[a]Mean ± SD. [b]Significantly different from group 1 by χ^2 test ($P<0.05$). [c]Significantly different from group 1 by Student's t-test ($P<0.05$). DH, dysplastic hyperplasia; PAP, papilloma; SCC, squamous cell carcinoma.

B. SD rat

Group	Treatment	No. of rats	Incidence			Multiplicity		
			Total	DH	PAP+SCC	Total	DH	PAP+SCC
1	4NQO	8	8	3	8	1.8±0.8[a]	2.0±1.4	1.5±0.8
2	4NQO→100 ppm nimesulide	10	10	2	8	1.6±0.7	1.3±0.6	1.5±0.8
3	4NQO→400 ppm nimesulide	10	10	2	8	1.3±0.7[b]	1.0±0.1	1.2±0.4
4	400 ppm nimesulide	5	0	0	0	0	0	0
5	None	5	0	0	0	0	0	0

[a]Mean ± SD. [b]Significantly different from group 1 by Student's t-test ($P<0.05$). DH, dysplastic hyperplasia; PAP, papilloma; SCC, squamous cell carcinoma.

of groups 1 ($P<0.001$) and 5 ($P<0.01$). Liver and relative liver weights of group 1 were significantly lower than that of groups 5 ($P<0.01$) and 3 ($P<0.01$), respectively. In Table II, the body weight of groups 1-3 was significantly lower than that of group 4 ($P<0.05$). Kidney and liver weights of group 1 and 3, respectively, were significantly lower than that of group 4 ($P<0.05$). Relative liver weight of group 2 was higher than that of groups 3 and 5 ($P<0.05$). These data indicate a toxic effect of 4NQO on the carcinogen-treated animals and that nimesulide may affect the weight of the body and the organs examined.

Occurrence of tongue lesions. On the time course study, an early induction of grossly visible tongue lesions including DH and tumor was found. These lesions were histopathologically DH, PAP and SCC (Fig. 2). After 3 weeks of 4NQO treatment, the incidence and number of DH in Hras128 rats markedly increased, and this increase persisted until the end of the experiment (at experimental-week 14) (Fig. 3A and C). In the DH lesion of Hras128 rats, treatment with 4NQO resulted in a 1.4- and 2.3-fold increase in incidence and number, respectively, when compared to the SD rats. At the experimental-week 14, the incidence and number of tongue tumors in the Hras128 rat were greater than that of the SD rat (Fig. 3B and D). Also, treatment of Hras128 rats with 4NQO resulted in a 2.7- and 4.3-fold increase in tumor incidence and number, respectively, when compared to the SD rats. At the end of the experiment, there was a significant increase in tumor multiplicity of the Hras128 rat (2.2±0.2) in comparison to the SD rat (1.5±0.8) ($P<0.05$). No visible esophageal tumors were found in any group of the Hras128 and SD rats.

Incidence and multiplicity of the tongue lesions. Treatment of Hras128 rats with 400 ppm nimesulide caused a significant and dose-dependent decrease in tumor incidence and total tumor multiplicity compared to group 1 ($P<0.05$, Table IIIA). In SD rats, the total tumor multiplicity was significantly decreased at 400 ppm nimesulide treatment ($P<0.05$, Table IIIB). In treatment of Hras128 and SD rats with nimesulide, the incidence and multiplicity were decreased in value but these changes were not statistically significant (Table III).

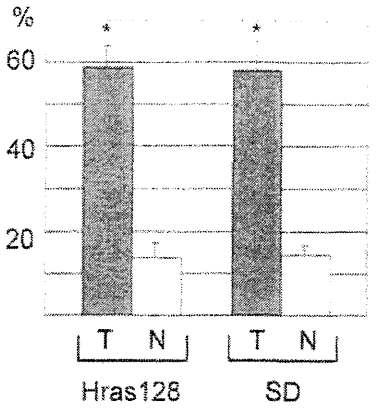

Figure 4. Proliferating cell nuclear antigen (PCNA) positive index in the tumor (T) and normal (N) tongue mucosa. Asterisks indicate significant difference in PCNA positive index between tumor and normal mucosa (Student's t-test, $P<0.05$). The difference was seen in both Hras128 and SD rats.

Positive index. To examine the effect of 4NQO in cell proliferation, we measured PCNA positive index in the tumor of group 1 and normal mucosa of group 5 (Fig. 4). In Hras128 rats, PCNA positive index was 58.8±4.9 (tumor) and 13.8±3.0 (normal mucosa). In SD rats, PCNA positive index was 58.1±6.6 (tumor) and 14.3±2.2 (normal mucosa). As shown in Fig. 4, treatment of Hras128 and SD rats with 4NQO caused a significant increase in PCNA positive index ($P<0.05$). These results indicate that treatment of rats with 4NQO increased cell proliferation in the tumor.

mRNA expression levels in the tumor of Hras128 rats. Because we found that at sacrifice the Hras128 rat developed greater number of tongue tumors than the SD rat and that 4NQO treatment enhanced cell proliferation in the tumor, we analyzed the levels of expression of cyclin D1, $p21^{CIP1}$, $p27^{KIP1}$, p53, COX2, using quantitative reverse transcription PCR (RT-PCR) assays. In tumor samples of the Hras128 rat, there was a marked (6.5- to 7.5-fold) and significant increase in the cellular levels of cyclin D1 and COX2 mRNA compared to the adjacent normal mucosa samples (Fig. 5). There was also a slight (1.7- to 2.3-fold) increase in those of p53 and $p21^{CIP1}$ mRNA (Fig. 5). We then examined whether nimesulide affects the levels of expression of these molecules in the tumors of Hras128 rats. Nimesulide caused a marked decrease in the cellular level of COX2, and also caused a slight decrease in that of cyclin D1 mRNA. Nimesulide treatment at high dose (400 ppm) inhibited the expression of COX2 mRNA to almost zero level. Nimesulide also caused a slight decrease in the cellular level of cyclin D1 mRNA.

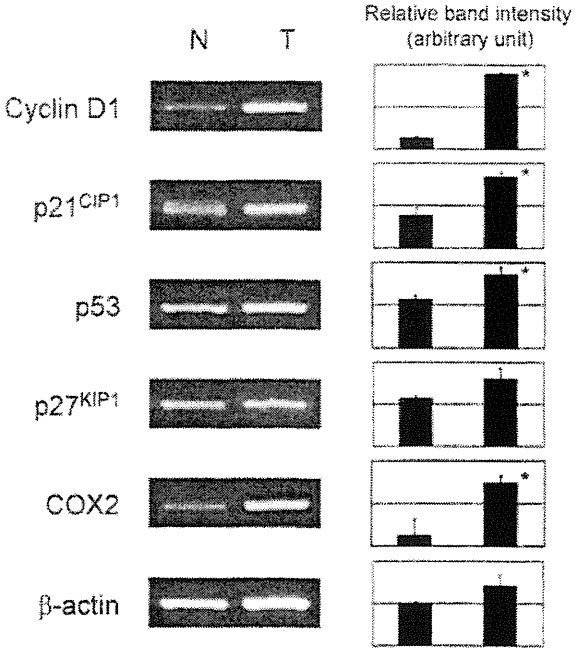

Figure 5. Representative results of RT-PCR assays. Densitometric analysis (right panel). Asterisks indicate significant difference between tumor (T) and adjacent normal mucosa (N) ($P<0.05$).

Discussion

Treatment of Hras128 rats with 4NQO caused an early induction (up to six experimental weeks) of DH and tumor in the tongue, when compared to the wild-type SD rat (Table III and Fig. 3). These results clearly show that Hras128 rats are more sensitive to 4NQO induced tongue carcinogenesis than SD rats. This susceptibility to a carcinogen is in accordance with previous experiments demonstrating that Hras128 rats are more sensitive to a 7,12-dimethylbenz[*a*]anthracene (DMBA) or 4NQO in the mammary or tongue tumors than were wild-type SD rats (11,21). In addition, Miyamoto *et al* demonstrated that the rasH2 mouse carcinogenesis model is highly susceptible to 4NQO induced tongue and esophageal tumors (12). In the present study, after three weeks of 4NQO treatment DH of the tongue epithelium in Hras128 rats markedly increased with respect to incidence and number, when compared with this lesion in SD rats (Fig. 3). The incidence and number of tongue tumors (PAP and SCC) also markedly increased after 6 weeks of 4NQO exposure, and this increase persisted until the end of the experiment (at experimental-week 14), when compared with these lesions in SD rats. In conventional 4NQO initiated carcinogenesis models, oral tumors are induced during 22-32 experimental weeks (11,22). In the present model, tongue tumors can be induced in only a short period of 14 experimental weeks. We therefore conclude that 4NQO-induced tongue carcinogenesis was extensively enhanced in the Hras128 rat.

Human oral cancer is a focal disorder (3), and experimental studies have indicated that there is a multistage process in the development of the oral lesions, in which dysplasias process to SCC through PAP (11,12). The results obtained in the present study showing that Hras128 and SD rats developed DH and tumors in a time-dependent manner (Fig. 3) is consistent with the established facts on human oral cancer. In addition, because of the ease of examining the lesions, the oral cavity is an excellent target organ for experimental studies. Therefore, the DH lesion may provide a useful biomarker for clarifying detailed carcinogenesis process and also provide clues to causative agents in human oral cancer.

The Ha-*ras* codon 12 and 61 mutations in human oral SCC occur at a frequency of approximately 35% (22). Previously we have reported that mutations in the *ras* family genes are 17% in 4NQO induced rat tongue tumors (23). The current Hras128 rats carry copies of the human c-Ha-*ras* transgene in their genome (15). The alkylating agent 4NQO is a powerful carcinogen in several organs (10), and it causes Ha-*ras* gene mutations by forming DNA adducts especially to guanine (N2, N7 and N8 positions) or adenine (N1 and N6 positions) (24-26). In a parallel study using Hras128 rats (unpublished data), no mutations were found in either endogenous rat c-Ha-*ras* gene or exogenous human c-Ha-*ras* gene in any tissue of DH, PAP SCC and normal mucosa, suggesting that in the present model the oral dysplasias progress to SCC via a mechanism, not involving mutational activation of the *ras* gene. In previous experiments, the transduced exogenous human c-Ha-*ras* gene was somatically mutated in the tumors of *N*-methyl-*N*-nitrosourea induced mammary carcinogenesis and *N*-butyl-*N*-(4-hydroxybutyl)nitrosamine induced urinary bladder carcinogenesis models (13,15). In these studies, however, no mutation was found in the endogenous gene. Similar results were also seen in a human c-Ha-*ras* transgenic mouse model (12). Therefore, it is likely that mutation in the transgene itself is not necessarily crucial for malignant progression and that these unique aspects in mutation status may reflect the different susceptibilities of different organs to specific carcinogens or the specificity of gene-carcinogen interactions. However, it remains to be determined whether the *ras* protein accumulates in the cytoplasm and nucleus of these tumors.

Overexpression of cyclin D1 has been found in both human and rat oral tumors (27,28). Overexpression of COX2 has been found in human oral cancer and DMBA induced hamster cheek pouch tumor (29,30). In the present study, we found that in tumor samples of Hras128 rats treatment of 4NQO caused a marked increase in the levels of mRNA expression of cyclin D1 and COX2, when compared to the adjacent normal mucosa (Fig. 5). We also found that treatment of 4NQO resulted in a significant increase in PCNA positive index in the tumor of Hras128 rats, when compared to the normal mucosa (Fig. 4). These analyses were performed in samples obtained at 14 weeks of the experiment. Thus, these results suggest that enhanced cell proliferation cooperates with the up-regulation of cyclin D1 and COX2 to cause a rapid induction of tongue tumors. We also found that mRNA expression levels of p53 and $p21^{CIP1}$ were marginally increased in the tumor of 4NQO-treated Hras128 rats (Fig. 5). This may be consistent with the study by Seo *et al* demonstrating that up-regulation of p53 and $p21^{CIP1}$ is a possible mechanism of nucleotide excision repair in response to 4NQO induced DNA damage (31).

The 4NQO-induced Hras128 rat oral carcinogenesis model may provide a system for evaluation of the mechanisms of multistage oral carcinogenesis and detection of causative agents in human oral cancer. Using this system, we also examined whether the model can be used to identify possible cancer preventive agents. A selective COX2 inhibitor, nimesulide (4-nitro-2-phenoxymethanesulphonanilide) was tested for its modifying effects on 4NQO-induced tongue carcinogenesis. We found that treatment of Hras128 rats with nimesulide caused a significant and dose-dependent decrease in tumor incidence and multiplicity compared to the control (Table IIIA). In Hras128 rats, treatment of nimesulide markedly decreased the level of expression of COX2 mRNA in the tumor compared to the adjacent normal mucosa. Therefore, the present model may also have some relevance and application to identify cancer preventive agents for human oral cancer. In summary, 4NQO rapidly causes dysplasia in oral squamous epithelia, which leads to PAP and SCC, as it does in human oral lesions. We consider the present Hras128 rat model a simple and rapid system that can be used for assessment of oral carcinogenesis and cancer prevention.

Acknowledgements

This study was supported by a Grant-in-Aid from the Ministry of Health, Labour, and Welfare of Japan, and a Grant-in-Aid from the Ministry of Education, Culture, Sports, Science and Technology of Japan.

References

1. Parkin DM, Bray F, Ferlay J and Pisani P: Global cancer statistics, 2002. CA Cancer J Clin 55: 74-108, 2005.
2. Stewart BW and Kleihues P: World Cancer Report, WHO Press, Lyon, 2003.
3. Smith CJ: Global epidemiology and aetiology of oral cancer. Int Dent J 23: 82-93, 1973.
4. Slaughter DP, Southwick HW and Smejkal W: Field cancerization in oral stratified squamous epithelium; clinical implications of multicentric origin. Cancer 6: 963-968, 1953.
5. Patel V, Leethanakul C and Gutkind JS: New approaches to the understanding of the molecular basis of oral cancer. Crit Rev Oral Biol Med 12: 55-63, 2001.
6. Davis S and Severson RK: Increasing incidence of cancer of the tongue in the United States among young adults. Lancet 2: 910-911, 1987.
7. Greenlee RT, Hill-Harmon MB, Murray T and Thun M: Cancer statistics, 2001. CA Cancer J Clin 51: 15-36, 2001.
8. Mackenzie J, Ah-See K, Thakker N, Sloan P, Maran AG, Birch J and Macfarlane GJ: Increasing incidence of oral cancer amongst young persons: what is the aetiology? Oral Oncol 36: 387-389, 2000.
9. Tanaka T, Kohno H, Sakata K, Yamada Y, Hirose Y, Sugie S and Mori H: Modifying effects of dietary capsaicin and rotenone on 4-nitroquinoline 1-oxide-induced rat tongue carcinogenesis. Carcinogenesis 23: 1361-1367, 2002.
10. Nakahara W, Fukuoka F and Sugimura T: Carcinogenic action of 4-nitroquinoline-N-oxide. Gan 48: 129-137, 1957.
11. Suzuki R, Kohno H, Suzui M, Yoshimi N, Tsuda H, Wakabayashi K and Tanaka T: An animal model for the rapid induction of tongue neoplasms in human c-Ha-ras proto-oncogene transgenic rats by 4-nitroquinoline 1-oxide: its potential use for preclinical chemoprevention studies. Carcinogenesis 27: 619-630, 2006.
12. Miyamoto S, Yasui Y, Kim M, Sugie S, Murakami A, Ishigamori-Suzuki R and Tanaka T: A novel rasH2 mouse carcinogenesis model that is highly susceptible to 4-NQO-induced tongue and esophageal carcinogenesis is useful for preclinical chemoprevention studies. Carcinogenesis 29: 418-426, 2008.
13. Asamoto M, Ochiya T, Toriyama-Baba H, Ota T, Sekiya T, Terada M and Tsuda H: Transgenic rats carrying human c-Ha-ras proto-oncogenes are highly susceptible to N-methyl-N-nitrosourea mammary carcinogenesis. Carcinogenesis 21: 243-249, 2000.
14. Asamoto M, Toriyama-Baba H, Ohnishi T, Naito A, Ota T, Ando A, Ochiya T and Tsuda H: Transgenic rats carrying human c-Ha-ras proto-oncogene are highly susceptible to N-nitrosomethylbenzylamine induction of esophageal tumorigenesis. Jpn J Cancer Res 93: 744-751, 2002.
15. Ota T, Asamoto M, Toriyama-Baba H, Yamamoto F, Matsuoka Y, Ochiya T, Sekiya T, Terada M, Akaza H and Tsuda H: Transgenic rats carrying copies of the human c-Ha-ras proto-oncogene exhibit enhanced susceptibility to N-butyl-N-(4-hydroxybutyl)nitrosamine bladder carcinogenesis. Carcinogenesis 21: 1391-1396, 2000.

16. Yoshida K, Tanaka T, Kohno H, Sakata K, Kawamori T, Mori H and Wakabayashi K: A COX-2 inhibitor, nimesulide, inhibits chemically-induced rat tongue carcinogenesis through suppression of cell proliferation activity and COX-2 and iNOS expression. Histol Histopathol 18: 39-48, 2003.
17. Banoczy J and Csiba A: Occurrence of epithelial dysplasia in oral leukoplakia. Analysis and follow-up study of 12 cases. Oral Surg Oral Med Oral Pathol 42: 766-774, 1976.
18. Kramer IR, Lucas RB, Pindborg JJ and Sobin LH: Definition of leukoplakia and related lesions: an aid to studies on oral precancer. Oral Surg Oral Med Oral Pathol 46: 518-539, 1978.
19. Suzui M, Inamine M, Kaneshiro T, Morioka T, Yoshimi N, Suzuki R, Kohno H and Tanaka T: Indole-3-carbinol inhibits the growth of human colon carcinoma cells but enhances the tumor multiplicity and volume of azoxymethane-induced rat colon carcinogenesis. Int J Oncol 27: 1391-1399, 2005.
20. Suzui M, Sunagawa N, Chiba I, Moriwaki H and Yoshimi N: Acyclic retinoid, a novel synthetic retinoid, induces growth inhibition, apoptosis, and changes in mRNA expression of cell cycle- and differentiation-related molecules in human colon carcinoma cells. Int J Oncol 28: 1193-1199, 2006.
21. Park CB, Fukamachi K, Takasuka N, Han BS, Kim CK, Hamaguchi T, Fujita K, Ueda S and Tsuda H: Rapid induction of skin and mammary tumors in human c-Ha-ras proto-oncogene transgenic rats by treatment with 7,12-dimethylbenz [a]anthracene followed by 12-O-tetradecanoylphorbol 13-acetate. Cancer Sci 95: 205-210, 2004.
22. Saranath D, Chang SE, Bhoite LT, Panchal RG, Kerr IB, Mehta AR, Johnson NW and Deo MG: High frequency mutation in codons 12 and 61 of H-ras oncogene in chewing tobacco-related human oral carcinoma in India. Br J Cancer 63: 573-578, 1991.
23. Suzui M, Yoshimi N, Tanaka T and Mori H: Infrequent Ha-ras mutations and absence of Ki-ras, N-ras and p53 mutations in 4-nitroquinoline 1-oxide-induced rat oral lesions. Mol Carcinog 14: 294-298, 1995.
24. Galiegue-Zouitina S, Bailleul B, Ginot YM, Perly B, Vigny P and Loucheux-Lefebvre MH: N2-guanyl and N6-adenyl arylation of chicken erythrocyte DNA by the ultimate carcinogen of 4-nitroquinoline 1-oxide. Cancer Res 46: 1858-1863, 1986.
25. Galiegue-Zouitina S, Bailleul B and Loucheux-Lefebvre MH: Adducts from in vivo action of the carcinogen 4-hydroxyamino-quinoline 1-oxide in rats and from in vitro reaction of 4-acetoxyaminoquinoline 1-oxide with DNA and polynucleotides. Cancer Res 45: 520-525, 1985.
26. Kohda K, Tada M, Hakura A, Kasai H and Kawazoe Y: Formation of 8-hydroxyguanine residues in DNA treated with 4-hydroxyaminoquinoline 1-oxide and its related compounds in the presence of seryl-AMP. Biochem Biophys Res Commun 149: 1141-1148, 1987.
27. Odajima T, Sasaki Y, Tanaka N, Kato-Mori Y, Asanuma H, Ikeda T, Satoh M, Hiratsuka H, Tokino T and Sawada N: Abnormal beta-catenin expression in oral cancer with no gene mutation: correlation with expression of cyclin D1 and epidermal growth factor receptor, Ki-67 labeling index, and clinicopathological features. Hum Pathol 36: 234-241, 2005.
28. Yoshida K, Tanaka T, Hirose Y, Yamaguchi F, Kohno H, Toida M, Hara A, Sugie S, Shibata T and Mori H: Dietary garcinol inhibits 4-nitroquinoline 1-oxide-induced tongue carcinogenesis in rats. Cancer Lett 221: 29-39, 2005.
29. Li N, Sood S, Wang S, Fang M, Wang P, Sun Z, Yang CS and Chen X: Overexpression of 5-lipoxygenase and cyclooxygenase 2 in hamster and human oral cancer and chemopreventive effects of zileuton and celecoxib. Clin Cancer Res 11: 2089-2096, 2005.
30. Pandey M, Prakash O, Santhi WS, Soumithran CS and Pillai RM: Overexpression of COX-2 gene in oral cancer is independent of stage of disease and degree of differentiation. Int J Oral Maxillofac Surg 37: 379-383, 2008.
31. Seo YR, Lee SH, Han SS and Ryu JC: Effect of p53 tumor suppressor on nucleotide excision repair in human colon carcinoma cells treated with 4-nitroquinoline 1-oxide. Res Commun Mol Pathol Pharmacol 104: 157-164, 1999.

Stat3 Orchestrates Tumor Development and Progression: The Achilles' Heel of Head and Neck Cancers?

M. Masuda*[,1], T. Wakasaki[1], M. Suzui[2], S. Toh[3], A.K. Joe[3] and I.B. Weinstein[3]

[1]*Department of Otorhinolaryngology and Head and Neck Surgery, Kyushu Koseinenkin Hospital, 2-1-1, Kishinoura, Nishiku, Kitakyushu 806-8501, Japan;* [2]*Laboratory of Medical Therapeutics and Molecular Therapeutics, Gifu Pharmaceutical University, 5-6-1, Mitahora-higashi, Gifu 502-8585, Japan;* [3]*Herbert Irving Comprehensive Cancer Center, College of Physicians and Surgeons, Columbia University MedicL Center, HHSC -1509, 701 W. 168th St., New York, 10032, USA*

Abstract: Despite recent advancements in treatment modalities, the overall survival and quality of life of patients with head and neck squamous cell carcinoma (HNSCC) have not significantly improved over the past decade. With the increasing emergency of new biological agents, the development of novel treatment schemes based on cancer cell biology may be promising for this group of patients. We previously introduced the "oncogene addiction" concept as a rationale for molecular targeting in cancer therapy and prevention. In this context, an increasing number of preclinical studies have demonstrated that the Signal Transducers and Activators of transcription 3 (Stat3) transcription factor play critical roles in the development and progression of a variety of tumors including HNSCC, by regulating cell proliferation, cell cycle progression, apoptosis, angiogenesis, immune evasion, Epithelial-Mesenchymal Transition (EMT) and through effects in cancer stem cells. The purpose of this review is to summarize current experimental and clinical evidence that suggests that HNSCC might be addicted to Stat3 and describes the molecular mechanisms that may explain this phenomenon. In addition, we discuss whether this addiction is an exploitable target for developing approaches for the treatment and prevention of HNSCC.

Keywords: Head and neck cancer, Stat3, molecular targeting, oncogene addiction, small molecule inhibitor.

INTRODUCTION

Multistage Carcinogenesis and the Concept of Oncogene Addiction in HNSCC

Head and neck squamous cell carcinoma (HNSCC) arises in the upper aerodigestive tract and is the sixth most common cancer worldwide [1]. Despite many recent advances in the treatment of cancers, the overall survival of patients with HNSCC has not significantly improved over the past decade [1]. In addition, treatment for patients with advanced stage disease remains largely dependent on radical surgery which often compromises major organs including the larynx, tongue, and pharynx, leading to substantial impairments in quality of life (QOL). The development and progression of HNSCC occur through a stepwise and progressive accumulation of genetic and epigenetic alterations mainly due to direct and repeated exposures to carcinogens including tobacco, alcohol, and viral infections [1-3]. Thus, HNSSC is a classical model of multistep carcinogenesis and field carcinogenesis, a concept originally proposed by Slaughter [4], that described a series of multifocal lesions within the same field [1-3]. In this genomic era, the design of novel treatment approaches that target these alterations may prove effective in the treatment and prevention of HNSCC.

During multistage carcinogenesis, the progressive accumulation of genetic alterations often leads to an extensive disruption in the genomic circuitry of the cell. However, despite the development of this "bizarre" circuitry, these cells remain addicted to the continued activity of only one or a few specific oncogenes for the maintenance of the malignant phenotype [5-7]. We have described this phenomenon as "oncogene addiction", and there are increasing number of preclinical and clinical reports that illustrate this concept, where the reversal of only one or a few of these abnormalities can profoundly inhibit the growth of cancer cells and in some cases lead to improved survival rates [5-7]. Thus, oncogene addiction supports the rationale for developing molecular targeting approaches in both cancer therapy and prevention. Related reviews based on this concept have recently been published [8, 9]. To date, the critical onogene (i.e., Achilles' heel) of HNSCC has not yet been identified.

Increasing number of studies have demonstrated that the Signal Transducers and Activators of transcription 3 (Stat3) transcription factor play significant roles in the development and progression of a variety of cancers including HNSCC, by regulating cell proliferation, cell cycle progression, cell survival (i.e., inhibition of apoptosis), angiogenesis, immune evasion and epithelial-mesenchymal transition (EMT) [10, 11]. Stat3 appears to be a critical molecule for the maintenance of the cancer phenotype in HNSCC, and therefore may represent the candidate oncogenes to which HNSCC is addicted. The purpose of this review is to summarize the current experimental and clinical evidence that supports the concept that HNSCC might be addicted to Stat3 signaling, and describe the molecular mechanisms that may explain this phenomenon. In addition, we discuss whether this addiction is an exploitable target for the prevention and treatment of HNSCC.

*Address correspondence to this author at the Department of Otorhinolaryngology and Head and Neck Surgery, Kyushu Koseinenkin Hospital, 2-1-1, Kishinoura, Nishiku, Kitakyushu 806-8501, Japan: Tel: +81-93-641-5111; Fax: +81-93-642-1868; E-mail: muneyuki.masuda@qkn-hosp.jp

1568-0096/10 $55.00+.00

EVIDENCE FOR STAT3 ADDICTION

Signal transducers and activators of transcriptions (STATs) comprise a family of cytoplasmic transcription factors (Stat1, Stat2, Stat3, Stat4, Stat5a, Stat5b, and Stat6) that were first identified as the key mediators of cytokine signaling by Darnell *et al.* in 1991 [12]. In normal cells, the activation duration of Stat3 in response to growth factors is transient and usually lasts from a few minutes to several hours [13]. Constitutive activation of Stat3 was first described in transformed cells as a consequence of the oncogenic tyrosine kinase v-Src. In 1996, Darnell and his colleagues demonstrated that introduction of a constitutively active mutant form of Stat3 into fibroblasts induced cellular transformation and these transformed cells were able to form tumors in nude mice, thus providing evidence that Stat3 is an oncogene [14]. Following this report, constitutive activation of Stat3 has been demonstrated in a variety of human cancer cell lines and clinical samples, and the multiple roles of this transcription factor in tumorigenesis and tumor progression have been intensively studied in rapidly expanding literature (for review, see ref. [11]). In HNSCC, constitutive activation of Stat3 was first demonstrated by Grandis *et al.* [15, 16]. They found that activation occurs early during HNSCC carcinogenesis due to the autocrine activation of TGF-α/EGFR signaling [15, 16], which is observed in a majority (80-100%) of HNSCC. [17-19]. We and other investigators have also demonstrated constitutive activation of Stat3 in primary HNSCC tissue specimens using immunohistochemistry or protein micro-arrays [20-23]. In addition to Stat3, activation of tumor suppressive Stat1 and oncogenic Stat5 has also been reported in HNSCC [11], but the roles of these two proteins are beyond the scope of this manuscript. Transfection of a constitutively active Stat3 construct in HNSCC cells resulted in increased proliferation *in vitro* and higher rates of *in vivo* tumor growth in mice [24], while inhibition of Stat3 using a dominant negative Stat3 construct, antisense oligonucleotides, a transcription factor decoy or siRNA led to decreased saturation density, increased serum dependence, growth inhibition and induction of apoptosis [15, 16, 20, 25-27]. In a xenograft model of HNSCC, administration of a Stat3 decoy or siRNA resulted in decreased tumor volume and induction of apoptosis [25, 26]. We and others [20, 22] found that Stat3 activation was significantly correlated with poor prognosis in the patients with squamous cell carcinoma of oral cavity. Taken together, these findings provide both laboratory and clinical evidence that HNSCC is significantly dependent on Stat3 signaling for the maintenance of the malignant phenotype, and thus might be addicted to Stat3.

MECHANISMS OF STAT3 ADDICTION (FIG. 1)

Diversity of Stat3 Activating Pathways in HNSCC

Activation of Stat3 signaling can occur through diverse nonspecific and HNSCC-associated pathways. As described above, Grandis *et al.* first reported that the frequent Stat3 activation in HNSCC occurs as a consequence of autocrine activation of TGF-α/EGFR signaling [15, 16]. In recent studies, Gutkind and his colleagues demonstrated that in a subset of HNSCC, autocrine activation and/or paracrine stimulation by IL-6 of the gp130/Jak pathway is primarily responsible for Stat3 activation rather than EGFR activation [28, 29]. In addition, they found that enhanced IL-6 secretion in HNSCC is dependent on NF-κB activity, suggesting the existence of cross-talk between the NF-κB and Stat3 signaling systems [29]. A recent study by Lee *et al.* also supports the relevance of IL-6 signaling in Stat3 activation in HNSCC [30]. In this study, hypermethylation (i.e., transcriptional silencing) of the Jak inhibitor, SOCS, and subsequent enhanced activation of Stat3 by IL-6 and gp130 were observed in about one third of HNSCC [30]. The non-receptor tyrosine kinase, Src, also plays a role in the activation of Stat3 in response to TGF-α stimulation [31]. Of note, Stat3 activation by TGF-α/EGFR, IL-6/gp-130/Jak or Src is not specific for the development of HNSCC, and a recent comprehensive review describes the interactions of these molecules in more detail [11].

Several investigators have recently identified Stat3 activating pathways, which appear to be highly associated with HNSCC carcinogenesis [21, 32, 33]. Arredondo *et al.* found that in oral keratinocytes, nicotine, a major carcinogen in tobacco, can activate Stat3 through the alpha 7 nicotinic acetylcholine receptor [32]. This tobacco-related Stat3 activation, at least in part, explains the markedly high rate of Stat3 activation (>80%) in clinical samples of oral squamous cell carcinoma that develop in tobacco-chewers [21]. It is now apparent that latent Epstein-Barr Virus (EBV) infection plays a critical role in the development of nasopharyngeal carcinoma, that displays unique biological properties among the HNSCCs [34]. Intriguingly, EBV infection of nasopharyngeal epithelial cells *in vitro* promoted activation of Stat3 and its downstream targets, providing the first report that Stat3 may mediate EBV-induced carcinogenesis in nasopharyngeal carcinoma [33]. Thus, it appears that constitutive activation of Stat3 in HNSCC can occur through diverse nonspecific and HNSCC-associated Stat3 activating pathways. The convergence of these diverse pathways on Stat3 activation suggests that Stat3 may be the oncogene to which HNSCC is addicted. A study by Kijima *et al.* further provides evidence that HNSCC may be addicted to Stat3 activation [24]. HNSCC cells that were transfected with a constitutively active Stat3 construct were no longer sensitive to either the growth enhancing effects of TGF-α or the growth inhibitory effects of an EGFR inhibitor [24]. This suggests that when Stat3 is constitutively and sufficiently activated by an alternative mechanism, the growth of these cells is no longer dependent on extrinsic Stat3 activating pathways. In other words, activation of Stat3, not the activation of EGFR, is the crucial driving force for cell proliferation. Therefore, the multiple and diverse Stat3 activating pathways appear to provide a safeguard for Stat3 activation, in case where one or a few pathways are lost with the genetic or epigenetic events that occur during tumor progression. In this context, direct inhibition and targeting of Stat3 will be a far more rational and powerful method for cancer prevention and therapy, rather than indirect inhibition of the multiple upstream Stat3 activating molecules (e.g., EGFR, Jak, Src). This aspect is discussed further in the targeting Stat3 section.

Effects of Stat3 Activation on the Expression of Cyclin D1 and c-myc

Over the past decade, it has become apparent that carcinogenesis is frequently associated with mutations or

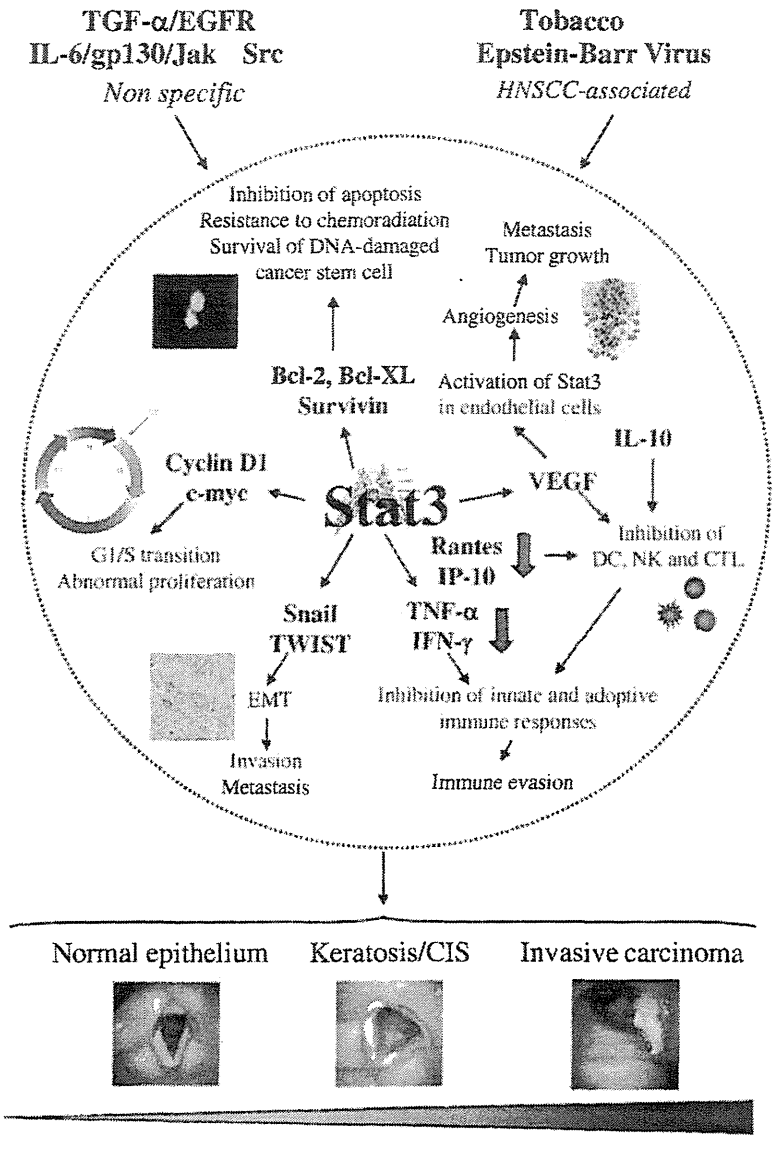

Fig. (1). A proposed mechanism by which HNSCC is addicted to Stat3.

Constitutive activation of Stat3 in HNSCC is caused by diverse signal transduction pathways. The frequent activation of TGF-α/EGFR in HNSCC was believed to be a major Stat3 activating pathway. However recent studies demonstrated that IL-6/gp130/Jak preferentially activates Stat3 in a subset of HNSCC. Src also plays causative roles in Stat3 activation. These Stat3 activating pathways are not HSCC-specific. On the other hand, recent findings displayed Stat3 activating mechanisms that are closely associated with HNSCC carcinogenesis. Tobacco or EBV latent infection activates Stat3 in oral keratinocyte or in nasopharyngeal epithelial cells. Stat3 transcriptionaly upregulates the levels of cyclinD1 and c-myc proteins, which result in the accerelated G1/S transition and abnormal proliferation. Anti-apoptotic proteins, Bcl-2, Bc-XL and survivin are also targets of Stat3. Overexpressions of these proteins inhibit apoptosis, promote cell survival and enhance cellular resistance for chemoradiation. Furthermore, it is proposed that these ani-apoptotic proteins protect DNA-damaged cancer stem cells from elimination by apoptosis and thereby allow them to expand clonally. In tumor cells, activated Stat3 enhances VEGF production and secretion. This VEGF, in turn activates Sat3 in endothelial cells, which is required for endothelial cell migration and therefore vessel formation. Consequent angiogenesis promotes tumor growth and metastasis. Stat3 is a negative regulator of both innate and adoptive immune responses. Tumor cells expressing constitutively active Stat3 produce markedly decreased levels of inflammatory cytokines, TNF-α, IFN-γ, RANTES and IP-10 and thereby inhibit both acute and adoptive immune responses. In addition, these tumor cells produce significantly increased levels of immunosuppressive cytokines and growth factors (e.g. VEGF and IL-10), which inhibit the functions of DCs, NK cells and CTLs. As a result, tumor cells with constitutive active Stat3 develop the state of "immune evasion". Recent findings suggest that Stat3 is involved in the process of EMT, at least in part, by activating Snail and TWIST. Tumor cells undergoing EMT acquire the ability to migrate and metastasize. Taken together, these findings indicate that Stat3 dominates (i.e. "orchestrates") the entire process of tumor development and progression of HNSCC.

abnormalities in the expression of various cyclins, CDKs and CDIs in a variety of human cancers including HNSCC [5]. In particular, the role of cyclin D1, which acts at the mid-portion of the G1-S transition, has been intensively studied in HNSCC [2, 35]. We and many others have demonstrated that the overexpression of cyclin D1 occurs in over 50 % of the cases of HNSCC and is a marker of poor prognosis in this disease [2, 35]. However, the cyclin D1 gene is amplified in only about 20% of the cases [2], and the mechanism of cyclin D1 overexpression is unclear in a majority of these cases. We previously found that the inhibition of Stat3 activity by a dominant negative Stat3 construct decreased cellular levels of cyclin D1 expression at the level of transcription [20]. In addition, in clinical samples of oral squamous cell carcinoma, there was a significant correlation between Stat3 activity and increased cyclin D1 expression [20]. These results provided the first evidence that in HNSCC constitutive activation of Stat3 may play a causative role in the overexpression of cyclin D1. This association was confirmed in several recent *in vitro* and *in vivo* studies [24, 26, 36, 37]. In addition, the significance of cyclin D1 in Stat3-dependent tumorigenesis was discovered in a recent study by Leslie *et al.* [38]. They found that cyclin D1 is required for Stat3-induced transformation (anchorage-independent growth) of immortalized fibroblasts. These findings, taken together with the fact that both the overexpression of cyclin D1 and the constitutive activation of Stat3 occur during relatively early phases of HNSCC carcinogenesis, suggest that cyclin D1 is a critical downstream target in the process of initial tumor development caused by Stat3.

The *c-myc* proto-oncogene encodes the c-myc transcription factor, and elevated or deregulated expression of c-myc has been detected in a wide variety of human cancers including HNSCC [39-41]. Overexpression of c-myc is associated with aggressive and poorly differentiated tumors and is therefore a marker of poor prognosis in patients with HNSCC [40, 41]. Although the precise mechanism of c-myc overexpression in HNSCC is not clear, it is now apparent that c-myc can be transactivated by Stat3 [11]. Indeed, EBV infection in nasopharyngeal epithelium can elevate the expression level of c-myc in a Stat3-dependent manner [33]. As seen in the pattern of cyclin D1 overexpression, c-myc overexpression also occurs during early stages of HNSCC carcinogenesis in an animal model of oral cancer [42] and in an *in vitro* transformation model of oral-esophageal cancer [43]. Thus, in HNSCC both c-myc and cyclin D1 appear to be crucial effecter proteins, that are active during the early phases of Stat3-induced tumorigenesis.

Effects of Stat3 Activation on Cell Survival (i.e. Inhibition of Apoptosis) and Sensitivity to Chemotherapy and Radiation Therapy

Sustained activation of Stat3 may lead to tumor promotion, in part, by upregulating the expression levels of two classes of anti-apoptotic protein family, the Bcl-2 family (e.g., Bcl-2, Bcl-XL and MCL-1) and the inhibitor of apoptosis (IAP) family (e.g., survivin) [11, 44]. Bcl-2 family proteins inhibit apoptosis by acting upstream of mitochondria prior to activation of caspases, while IAP family proteins exert their effects after caspase activation [44]. Deregulated expression of these anti-apoptotic proteins can protect cancer cells from apoptosis and allow them to survive during tumor progression [44]. In addition, overexpression of these proteins may prevent apoptosis following treatment with conventional DNA-damaging cancer therapies (i.e., chemotherapy and radiation), thus significantly decreasing cellular sensitivity of cancer cells to these therapies [44]. Indeed, both precursor and established lesions of HNSCC display frequent overexpression of Bcl-2, Bcl-XL or survivin and this overexpression is significantly associated with aggressive phenotype (i.e., advanced TNM stage) [45-48]. Overexpression of Bcl-2 or Bcl-XL is also correlated with poor prognosis in early stage HNSCC after treatment with radiation [48, 49]. However, it should be noted that other investigators reported a paradoxical association between increased Bcl-2 expression and favorable outcome in patients with HNSCC [47, 50]. Increased survivin expression was significantly associated with aggressive phenotype, presence of nodal and distant metastases, and poor clinical outcome in HNSCC [51-54]. The association between survivin and tumor metastases is consistent with a recent theory, which proposes that cancer stem cells are protected from apoptotic elimination by virtue of anti-apoptotic proteins and are thereby allowed to expand clonally until they acquire metastatic ability [55, 56]. This concept will be discussed in more detail in the Effects of Stat3 Activation and EMT and cancer stem cells section.

The important roles of Stat3 in regulating anti-apoptotic proteins have been demonstrated in both HNSCC cancer development and treatment. Stat3-induced expression of Bcl-XL was observed after both EBV-infection of nasopharyngeal epithelium and stable expression of constitutively activated Stat3 in HNSCC [24, 33]. Conversely, inhibition of Stat3 activity by a dominant negative Stat3 construct, antisense oligonuculeotides, decoy oligonuculeotides and siRNA led to decreased levels of Bcl-2, Bcl-XL and survivin, inhibition of tumor growth and induction of apoptosis [16, 20, 25-27, 36]. Treatments of laryngeal cancer cells with sulindac, a nonsteroidal anti-inflammatory drug induced apoptosis and growth inhibition *in vivo* due to decreased survivin expression caused by the downregulation of Stat3 [57]. We and other investigators found that inhibition of Stat3 markedly enhanced *in vitro* and *in vivo* sensitivity of HNSCC cells by down-regulating Bcl-2 and Bcl-XL expression to the chemotherapeutic agents, 5-fluorouracil and cisplatinum [36, 58]. It was also demonstrated that indirect inhibition of Stat3 by EGFR inhibitor can significantly promote sensitivity of HNSCC cells to radiation [59, 60].

Effects of Stat3 Activation on Angiogenesis

Angiogenesis, the recruitment of new capillaries from existing vessels, is indispensable during the processes of tumor development, three dimensional tumor growth, and metastasis of solid tumors including HNSCC [61-63]. To date, several angiogenic factors have been identified. Among them vascular endothelial growth factor (VEGF) is one of the most prominent mitogens for endothelial cells, and the role of VEGF in carcinogenesis has been extensively investigated [62, 64]. Elevated VEGF production has been associated with both higher levels of intratumoral microvessel density (IMVD) and poor prognosis in the patients with several ma-

lignancies including HNSCC [65-69]. The precise mechanism by which VEGF is overexpressed in HNSCC is not known. In our previous *in vitro* study, we found that Stat3 directly activates VEGF production *via* a putative Stat3 responsive element (-849 to -842) on the VEGF promoter [70]. Furthermore, in clinical samples of oral HNSCC, we found significant correlations between Stat3 activity, VEGF production, and angiogenesis [70]. These findings are consistent with a recent study by Xi *et al.* [36], according to that administration of a Stat3 decoy significantly decreased the expression level of VEGF and thereby inhibited tumor growth and angiogenesis in a xenograft model of HNSCC. Furthermore, in endothelial cells the activation of Stat3 signaling by VEGF is required for both migration and vessel formation [71]. Thus in HNSCC angiogenesis, Stat3 appears to have at least two different functions: Stat3 enhances VEGF production by HNSCC cells and this VEGF, in turn, promotes Stat3 activity in endothelial cells, required for angiogenesis.

Effects of Stat3 Activation on Immune Evasion

Previous studies suggest that tumors including HNSCC can escape from rejection by both innate and adoptive immune responses through "immune evasion" or " immune tolerance" [72, 73]. It has been shown that tumor "toleration" is an active process caused by tumor cells resulting from imbalances in the tumor microenvironment, including alterations in antigen-presenting-cell subsets (e.g., dendritic cells (DC)), in co-stimulatory and co-inhibitory molecules and in ratios of effecter (e.g., NK and CTL) and regulatory T cells [72, 73]. Interestingly, Stat3 may negatively regulate these inflammatory responses. Mice whose macrophages and neutrophils are devoid of the Stat3 gene develop chronic enteritis, and $Stat3^{-/-}$ macrophages can restore the responsiveness of tolerant CD^{4+} T cells and reverse systemic tolerance [74, 75]. Recent studies have demonstrated that constitutive activation of Stat3 in both tumor cells and components of the host immune system may cooperate to impair both innate and adoptive immune responses to tumors [76-78]. Tumor cells expressing constitutively active Stat3 produce markedly decreased levels of TNF-α, IFN-γ, RANTES and IP-10, which results in the inhibition of acute inflammatory responses and decreased migration and infiltration of neutrophils, macrophages, and T-cells into the tumor site [73, 77, 78]. These tumor cells also produce increased levels of immunosuppressive cytokines and growth factors (e.g. VEGF and IL-10) [73, 78], that, in turn, activate Stat3 in immature DCs, and block DC differentiation [76, 78]. The subsequent lack of mature antigen-presenting DCs results in T-cell tolerance to tumor antigens [73, 78]. Taken together, tumor cells with constitutive activation of Stat3 exert multiple effects on the host immune system that lead to immune evasion and the subsequent development of human cancers, including HNSCC. The roles of Stat3 in HNSCC immune evasion are comprehensively described in a recent review [73].

Effects of Stat3 Activation on EMT and Cancer Stem Cell

At the final step of malignant tumor progression, epithelial tumors including HNSCC acquire the ability to metastasize distant organs - this is often accompanied by a process known as Epithelial-Mesenchymal Transition (EMT) during which cancer cells change from a highly differentiated, epithelial morphology to a migratory invasive phenotype [79, 80]. During EMT, epithelial cancer cells undergo down-regulation of apical and basolateral adherent molecules including E-cadherin and cytokeratins and upregulation of mesenchymal molecules including vimentin and N-cadherin, thereby losing cell-cell contact and gain the cell motility [79, 80]. It was recently shown that Stat3 activation is essential for EMT in the zebrafish gastrula organizer [81]. In this system, Stat3 upregulated a zinc transporter protein, LIV-1, which functions as a nuclear transporter of the zinc-finger protein Snail, a master regulator of EMT [81]. Yang *et al.* found that Stat3 activation plays an important role in TGF-β-mediated EMT [82], while Lo *et al.* showed that Stat3 mediates EGF/EGFR-induced EMT by upregulating the expression of TWIST [83]. The results of these studies strongly suggest that Stat3 may be an important regulator of EMT and tumor progression. Of note, Stat3 activation and EMT have not been studied in HNSCC yet.

As described in a recent review, the concept of EMT and the cancer stem cell theory contribute importantly to distinct features of carcinogenesis - the existence of heterogeneous cell populations in a single tumor and the dynamically changing phenotypes displayed by individual cancer cells during EMT or MET [56]. Thus, in addition to the diverse functions of Stat3, that we have described in this review, we hypothesize that Stat3 might also be a master regulator of cancer stem cell development in HNSCC. A recent study of skin carcinogenesis provided a striking example that may confirm this hypothesis. In this model, the investigators demonstrated that Stat3 is required for the *de novo* epithelial carcinogenesis and maintained the survival of DNA-damaged stem cells. By upregulating Bcl-XL, cyclin D1 and c-myc, Stat3 induced the cell proliferation required for clonal expansion of initiated cells during tumor promotion [55]. This finding is not surprising when we think of the fundamental roles of Stat3 in normal cell physiology. During gastrulation, organogenesis, and wound healing, this latent cytoplasmic transcription factor is transiently activated in embryonic precursor cells or in normal somatic stem cells only during specific events, when this activation is required [84-86]. Thus, if stat3 was abnormally and constitutively activated in normal somatic stem cells in the upper aerodigestive epithelium, this activation could lead to the development of cancer stem cells in this tissue, as seen with the abnormal expression of β-catenin during colon carcinogenesis [56, 79, 87].

In summary, it is quite surprising that activation of a single transcription factor is profoundly associated with the diverse steps that are critical for the development and progression of HNSCC. These findings strongly suggest that HNSCC is addicted to the activation of Stat3, and therefore, this activation might be the Achilles' heel of HNSCC. A proposed mechanism by which HNSCC is addicted to Stat3 is summarized in Fig. (1).

TARGETING STAT3

A successful and feasible molecular targeting approach must fulfill several criteria: (1) the particular cancer is highly dependent on (i.e., addicted to) the targeted molecule, (2) the

potential for escape from the given state of oncogene addiction is low, (3) strategies for targeting the particular oncogene are clinically available, and (4) treatment with the targeted agent is associated with minimal or tolerable toxicity. The evidence for Stat3 addiction in HNSCC (criterion 1) has been discussed in the preceding sections. In this section, we will discuss whether Stat3 targeting can fulfill the remaining criteria.

Escape from the State of Oncogene Addiction

As already described in our previous review, cancers can potentially escape from a given state of oncogene addiction [7]. For example, in the Her-2/neu breast cancer model, tumors that recurred after treatment with trastuzumab were found to be Her-2/neu independent. These tumors contained increased expression of the transcription factor Snail, suggesting that recurrent tumors escaped from the addiction to Her-2/neu and were secondary addicted to Snail [7]. However, this finding may also suggest that the activation of Her-2/neu is required during the early phase but not in the advanced phase (i.e., recurrence) of tumor development; for Snail the converse would be true. Thus, activation of these two genes may play critical and transient roles during particular stages of breast tumor development and progression. In contrast, as we have discussed in this review (Fig. **1**), the activation of Stat3 appears to "orchestrate" the entire process of HNSCC development and progression. Therefore, it would be quite difficult for HNSCC to completely escape from the addiction to Stat3. On the other hand, HNSCC could escape from the influences of Stat3 targeted downstream genes (i.e., cyclin D1, Bcl-XL or VEGF) during particular stages of carcinogenesis. In this model, the potential for escape from Stat3 addiction would be low (criteria 2). However, it should be noted that activation of the transcription factor NF-κB might provide an additional target in HNSCC, since these two transcription factors transactivate a surprisingly overlapping set of downstream molecules (e.g., c-myc, cyclin D1, Bcl family proteins, IAPs and VEGF) in HNSCC, as summarized in our recent study [88]. Theoretically, combined inhibition or targeting of Stat3 and NF-κB might exert synergistic activity against HNSCC. This possibility remains to be analyzed in future *in vitro* and *in vivo* studies.

Strategies for Targeting Stat3

A considerable number of strategies can be effective for the inhibition or targeting Stat3. These strategies are generally divided into three categories based on their mechanisms of action: (1) indirect stat3 inhibition following the inhibition of Stat3 activating molecules (e.g., EGFR, Jak and Src) or the activation of Stat3 inhibiting molecules (e.g., SOCS and IAST), (2) direct inhibition of Stat3, and (3) unknown or non-specific mechanisms (i.e., mechanisms of action are not clearly elucidated or difficult to categorize). These strategies including particular compounds have been described in several recent reviews [11, 89-91]. Cucurbitacin I, a selective Jak inhibitor, and indirubin, a Chinese herb constituent, can indirectly inhibit Stat3 by inhibiting the kinase activity of Jak or Src [92, 93]. We previously demonstrated that the green tea compound EGCG can inhibit the activation of Stat3 in HNSCC by inhibiting TGF-α/EGFR/erbB2 signaling, thus, providing another example of indirect Stat3 targeting [94]. On the other hand, direct inhibition of Stat3 may provide a more powerful and efficient strategy of Stat3 inhibition, since Stat3 activity can be maintained by multiple and diverse activating pathways as described in the Diversity of Stat3 activating pathways in HNSCC section. Until recently, methods for direct inhibition were limited mainly to genetic approaches using dominant negative constructs, antisense and decoy oligonucleotides or siRNA. Although these methods of "gene therapy" are powerful and reliable tools for *in vitro* or animal studies, their potential for clinical use remain much less clear. By contrast, the recent clinical success of using small molecule inhibitors like imatinib, which directly targets the BCR-ABL protein in CML, strongly supports the great potential for using molecular targeting drugs in cancer therapy [95]. In this context, investigators have recently discovered direct small molecule Stat3 inhibitors, STA-21, Stattic, and 531-201, which directly bind to the SH-2 domain of Stat3 and thereby inhibit Stat3 dimerization. These agents were identified using powerful structure-based virtual screening or high-throughput screening and fluorescence polarization assays [96-98]. These compounds strongly inhibited the growth of and induced apoptosis in breast carcinoma cells, which displayed constitutive activation of Stat3, while sparing normal fibroblast or carcinoma cells in which Stat3 is not activated [96-98]. Furthermore, S31-201 inhibited the growth of human breast carcinomas *in vivo* [98]. These studies provide support for the design of future Phase 1 clinical studies and strategies for the clinical targeting of Stat3 (criterion 3).

Possible Toxicity with Stat3 Inhibition

It is well known that Stat3 activation is required during early development, since Stat3-null mice display an embryonic-lethal phenotype [11]. On the other hand, non-tumor cells can proliferate and survive *in vitro* and *in vivo* following tissue specific knock-out of Stat3 [11]. In addition, numerous experimental studies demonstrated that growth inhibition or apoptosis caused by the inhibition of Stat3 is observed specifically in cancer cells, which display constitutively active Stat3, while sparing normal and cancer cells that do not overexpress Stat3 [11]. These findings might suggest that clinical therapy with Stat3 inhibitors may not be associated with serious systemic toxicity. However, in view of the fact that Stat3 is a ubiquitous transcription factor, this expectation is likely optimistic. Recent advancements in drug delivery systems, in particular, those based on nanomedicine, might be of great importance in reducing possible toxicities associated with Stat3 targeting, by allowing tumor-specific delivery of a small molecule Stat3 inhibitor [99]. Thus, these approaches may be used to develop agents that specifically target Stat3-addicted cancers while sparing normal, non-addicted tissue (criterion 4).

CONCLUSIONS AND FUTURE DIRECTIONS

The diverse functions of Stat3 appear to be essential in a variety of processes, which are highly associated with tumor development and progression of HNSCC. In addition, the recent discovery of small molecule Stat3 inhibitors might